Economic Geology
Vol. 88, 1993, pp. 733–753

SOCIETY OF ECONOMIC GEOLOGISTS

Holly Huyck and Richard Grauch
SEG Newsletter Editors
5808 South Rapp Street, Suite 209
Littleton, Colorado 80120
Telephone and FAX (303) 988-1124

SEG Distinguished Lecture

The Evolution of Magmatic Fluids in the Epithermal Environment: The Stable Isotope Perspective*

ROBERT O. RYE

U. S. Geological Survey, Mail Stop 963, Denver Federal Center, Denver, Colorado 80225

Introduction

Through the years I have studied a number of epithermal ore deposits that were related to silicic magmatism (Rye, 1966; Landis and Rye, 1974; Rye and Sawkins, 1974; Rye et al., 1974, 1992; Kelly and Rye, 1979). Frequently, magmatic fluids were clearly the dominant component of the hydrothermal systems responsible for these shallow deposits. Stable isotope studies of such systems, when supported by detailed geologic framework studies and fluid inclusion and other geochemical data, not only identify magmatic fluid components but also place important constraints on their evolution in the system. My purpose today is to construct a simple model that summarizes some of the fundamental processes that govern the evolution of magmatic fluids which reach the epithermal environment. This model will be consistent with the stable isotope geochemistry of five individual deposits: Julcani, Peru; Summitville, Colorado; Alunite Ridge near Marysvale, Utah; Red Mountain near Lake City, Colorado; and Providencia, Mexico. Each deposit will illustrate a different aspect of high-level magmatic fluid evolution. Discussion of each deposit will be brief because my primary purpose is to focus on fundamental processes rather than on the details of individual deposits. These deposits have been investigated in my laboratory with colleagues, post-docs, and students over a number of years. My coworkers, whom I shall acknowledge at appropriate places, introduced me to the areas and provided the geologic and often much of the geochemical framework, both of which are critical to proper interpretation of stable isotope data. Without their contributions I would not be giving this talk.

Models and Principles of Interpretation of Stable Isotope Data of Magmatic Fluids

Important elements of magmatic fluid systems

Before discussing the individual deposits we need to review some of the general processes that affect fluids after their exsolution from a magma and some of the principles of stable isotope geochemistry that are used in interpretations. The cartoon in Figure 1 portrays the early stages of a hypothetical magmatic hydrothermal system related to an I-type magma underlying a volcanic dome field. Many people have contributed to our knowledge of the geochemical, geophysical, and geometric relationships of such systems (e.g., Lister, 1974, 1980; Henley and McNabb, 1978; Burnham, 1979; Fournier, 1983, 1985, 1987, 1991, 1992; Henley and Ellis, 1983). I am particularly indebted to Bob Fournier for pointing out to me the importance of the brittle-ductile transition which often occurs at about 400°C in these systems. Exsolved magmatic fluids which concentrate in the fluid-rich carapace of the magma probably have initial salinities between 10 and 30 percent (Fournier, 1987, 1992) and chemical and isotopic compositions determined by equilibration with the magma. The part of the system of critical importance to epithermal ore deposits is the deep crystalline rocks between the brittle-ductile transition and the water-

* Delivered before the Society of Economic Geologists at their meeting with the Geological Society of America, October 27, 1991, in Cincinnati, Ohio.

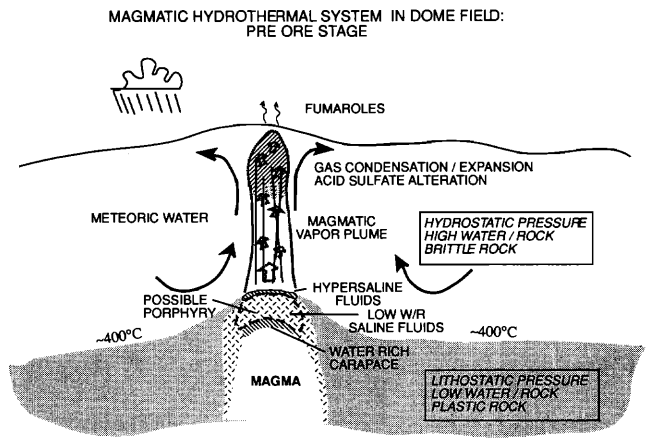

FIG. 1. Model showing early stages of a high-level magmatic hydrothermal system underlying a volcanic dome field and the relationship of fluid elements to the water-rich carapace of the magma and the brittle-ductile transition which usually occurs about 400°C in these systems (Fournier, 1987, 1992). This stage is characterized by a vapor plume and a counterpart hypersaline brine at deep levels in the hydrostatic environment of the system. Dashed area is source of evolved magmatic fluids for epithermal ore deposits. The water-saturated carapace is envisioned as defined by Burnham (1979).

rich carapace of the magma. These rocks behave quasiplastically such that brittle fracture is difficult, fractures that do occur are quickly sealed, and penetration by meteoric water is minimized. Under these conditions fluid pressures will be lithostatic, water-rock ratios will be low, and the isotopic and chemical characteristics of magmatic fluids which leave the water-rich carapace will be governed by equilibration with the rocks. These deep crystalline rocks may or may not be the site of porphyry-type mineralization and alteration. Above the brittle-ductile transition, magmatic fluids will encounter fractures that may be open to the surface. Here fluid pressures approach hydrostatic, meteoric water circulation is common, water-rock ratios of the system can be large, and evolved magmatic fluids may be out of isotopic and chemical equilibrium with the rocks. In this environment a vapor plume may rise from the brittle-ductile transition and result in acid sulfate alteration at high levels. As Fournier (1987, 1992) has pointed out, this vapor plume may overlie a residual hypersaline brine near its base at the brittle-ductile transition. If the fluid pressure in the deep crystalline rocks were suddenly to become hydrostatic in the later stages of the system, these hypersaline liquids as well as deeper saline liquids could be released with enough energy to ascend rapidly to high levels. I will come back to this cartoon and present an additional one for the later ore-bearing stage at the end of the talk.

My general message is that saline magmatic fluids which produce epithermal ore deposits are chemically decoupled from the carapace of the magma and are derived from the area between the water-rich carapace and the brittle-ductile or lithostatic-hydrostatic transition. The ore fluids ascend from this crystalline rock environment at such high rates that their deep-seated isotopic and chemical characteristics are largely preserved at high levels. These ore fluids may make their appearance at high levels after the development of one of two types of acid vapor plumes whose fluids ascend from the brittle-ductile transition.

Interpretation of hydrogen and oxygen isotope data for magmatic fluids

Most of us are familiar with the principles used for the interpretation of data on the isotopic composition of water in magmatic fluids (Ohmoto, 1986). The δD and $\delta^{18}O$ values of water of primary magmatic fluids can easily be calculated from the composition of unaltered biotite in cogenetic igneous rocks (Fig. 2). These values will both decrease substantially along the exchange track shown by the solid squares if the fluid exchanges with deep crystalline rocks at submagmatic temperatures (Ohmoto and Rye, 1974). By the time the temperatures of fluids drop below 700°C, they have probably left the water-rich carapace of the magma and reside in crystalline rocks. A number of processes occurring near the carapace of the magma such as H_2 loss from the system (Carten et al., 1988), degassing of the magma chamber (Taylor et al., 1983), incorporation of meteoric water in the magma chamber or overlying roof rocks (Lipman and Friedman, 1975; Taylor, 1986), and possibly high-temperature phase separations of exsolved saline magmatic fluids can also effect the isotopic composition of primary magmatic fluids. However, fluid iso-

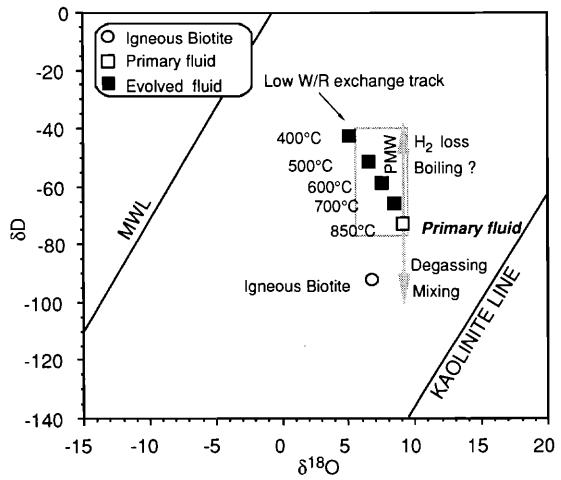

FIG. 2. Principles governing the isotopic composition of magmatic fluids after exsolution from magma. The primary fluid composition is calculated from primary igneous biotite at the temperature of crystallization. The exchange track is calculated as in Ohmoto and Rye (1974) for felsic rocks having compositions compatible with that of the biotite. This exchange track shows the change in composition for fluids in the low water-rock environment between the water-saturated carapace of the magma (T ~850°C) and the brittle-ductile transition (T ~400°C). Changes in magmatic fluid compositions due to degassing of magma chamber, loss of hydrogen from magma chamber, incorporation of meteoric water, and saline fluid-phase separations are indicated qualitatively by the arrows.

tope compositions will always end up somewhere along the exchange track if the fluids exchange with crystalline rocks in the low water-rock environment below the brittle-ductile transition. As we examine individual deposits, you will notice that their deep fluids will have isotope compositions close to the low-temperature end of the exchange track in every instance where the track can be calculated. Remember also that the primary magmatic water box (PMW in Fig. 2) is only a conventional reference (Taylor, 1979). The composition of magmatic waters from a given area may fall outside of the box (cf. Matsuhisa, 1992; Taylor, 1992) and waters of other origins may have compositions that fall within the box.

Evolution of H_2S/SO_2 in magmatic fluid systems

In order to interpret sulfur isotope data on magmatic fluid systems we need to review some of the factors that govern the ratio of the reduced to oxidized sulfur species in the fluids (Ohmoto and Rye, 1979; Burnham and Ohmoto, 1980). The standard f_{O_2}-T diagram in Figure 3 shows three hypothetical cooling trajectories for fluids exsolved from a typical I-type magma. Fluids exsolved from such magmas may initially lie on either side of the H_2S/SO_2 line. Fluids which leave the magma and cool without reacting with the wall rocks may be internally buffered and follow the trajectory of constant H_2S/SO_2. However, the same fluids are likely to follow a rock buffer trajectory and become H_2S dominant if they react with crystalline rocks below the brittle-ductile transition. A possible third path was suggested to me by Terry Gerlach. As we shall see, if the system is suddenly decompressed, magmatic fluids may become SO_2 rich because of low-pressure shifts in high-temperature gas equilibria (Gerlach, 1993). In real life the actual path a given fluid follows may be quite complicated, involving combinations of these possibilities.

Interpretation of $\delta^{34}S$ data of sulfur-bearing minerals in magmatic fluid systems

We can sometimes trace the oxidation path of the fluids by comparing the $\delta^{34}S$ values of the sulfur-bearing minerals in the veins with those in presumably cogenetic igneous rocks (Fig. 4). If the bulk composition of sulfur in the system remains constant, the time-space sulfur isotope systematics of vein minerals will reflect only the changes in temperature and oxidation state of the fluids after their exsolution from the magma (Ohmoto and Rye, 1979). If the oxidation state of fluids changes dramatically after their exsolution, the $\delta^{34}S$ values for different generations

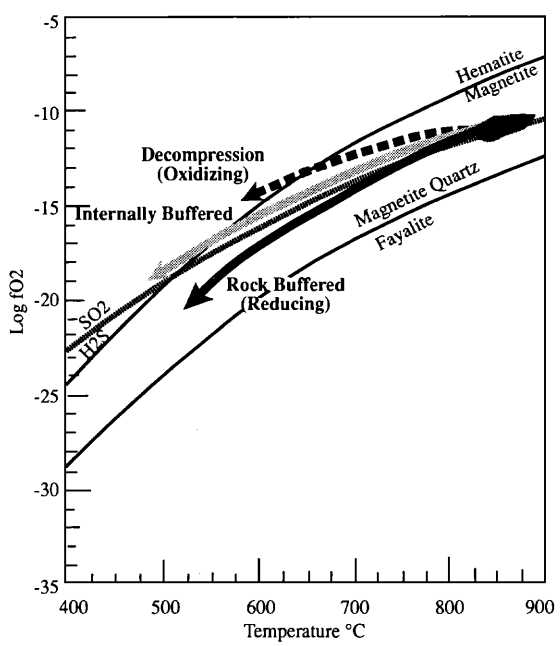

FIG. 3. Three hypothetical paths of H_2S/SO_2 of hydrothermal fluids after their exsolution from I-type magmas having temperature $-f_{O_2}$ shown by the irregular area that straddles the H_2S/SO_2 = 1 line. Below 400°C SO_2 will disproportionate according to the reaction $4SO_2 + 4H_2O = 3H_2SO_4 + H_2S$. Modified from Ohmoto and Rye (1979) and Ohmoto (1986). Paths are drawn schematically. For examples of calculated paths see Deen (1990).

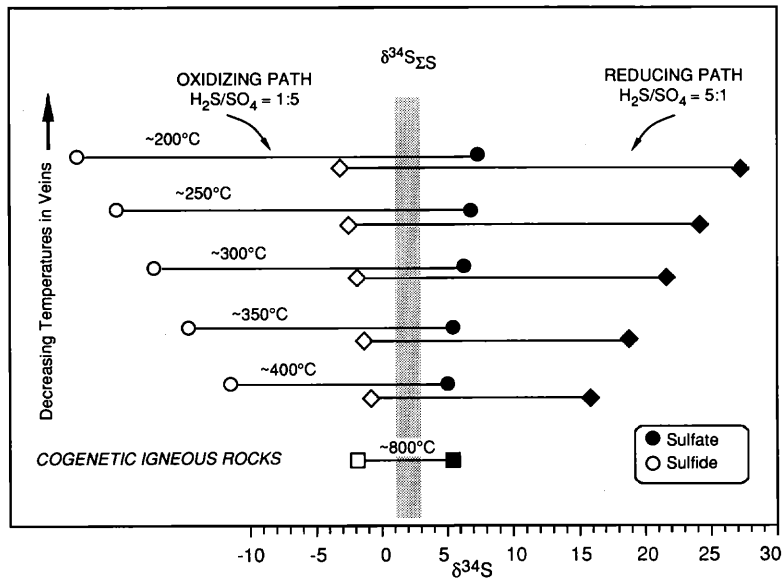

FIG. 4. Idealized $\delta^{34}S$ systematics of coexisting sulfides and sulfate vein minerals derived from evolved magmatic fluids with initial $H_2S/SO_2 = 1$ and precipitated over the temperature range 400° to 200°C. The diagram takes into account the effect of the disproportionation of SO_2 at about 400°C on the $\delta^{34}S$ values of the minerals. Diamonds show fluids which followed a reducing path. Circles show fluids which followed an oxidizing path. If the $\delta^{34}S_{\Sigma S}$ of the system remains constant, its value must be between the values for sulfate and sulfide in the cogenetic igneous rocks and is here assumed to be 2 ± 1 per mil.

of coexisting vein sulfate and sulfides will also shift dramatically with respect to those values for sulfate and sulfides in cogenetic igneous rocks.

As shown in Figure 4 the $\delta^{34}S$ values of bulk sulfur in the system must lie between the $\delta^{34}S$ values for sulfate and sulfide in the igneous rocks. The $\delta^{34}S$ value for the bulk sulfur in the magma and the sulfur speciation of the hydrothermal fluids during exsolution from a magma can also be calculated by applying thermodynamic data which relate f_{O_2} and temperature to mineral assemblages of cogenetic igneous rocks (Ohmoto, 1986; Drexler and Munoz, 1988; Whitney, 1988). We can observe the evolution of $\delta^{34}S$ values of vein sulfate and sulfides that precipitated from fluids that became more oxidizing or reducing than primary magmatic fluids. The important observation is the mass balance shift. For example the $\delta^{34}S$ values of vein sulfates that precipitate from fluids which follow a reducing path become much larger than those for the igneous sulfate whereas the values for vein sulfides remain close to those for the igneous sulfide. The opposite is true for fluids that follow an oxidizing path. We will see examples of both reducing and oxidizing fluid paths in our discussion of individual deposits.

Interpretation of $\delta^{34}S$ and $\delta^{18}O_{SO_4}$ values of magmatic hydrothermal and magmatic steam alunites

Two different types of alunite can form from magmatic vapor fluids (Rye et al., 1992) and their stable isotope systematics are shown in Figure 5. The most common type is magmatic hydrothermal alunite that forms during the disproportionation of SO_2 in condensed magmatic vapor. These alunites coexist with pyrite and have equilibrium sulfur and oxygen isotope values. When fluid compositions are constant, their data sets will reflect the changes in oxidation state and temperature in the fluids. These alunites may form from fluids that followed any of the three paths shown previously in Figure 3. The temperature scale and appropriate trend of isotope values for a given set of conditions in Figure 5 can be used as a reference in all of the subsequent sulfur and oxygen isotope diagrams for these alunites. Magmatic steam alunites are much rarer and are believed to form during the expansion of rapidly ascending SO_2-rich magmatic vapor fluids that followed the oxidizing, decompression path shown previously. These alunites do not coexist with pyrite and are characterized by near-equilibrium $\delta^{18}O$ values but by disequilibrium $\delta^{34}S$ values that are nearly the same as the bulk sulfur in the fluids. We will observe examples of each type of alunite and the reactions leading to their formation in our discussion of individual deposits.

Equilibration rates of aqueous sulfur species in low pH fluids

The experimental work of Ohmoto and Lasaga (1982) indicates that the time to obtain sulfur isotope equilibrium between aqueous sulfate and sulfide in

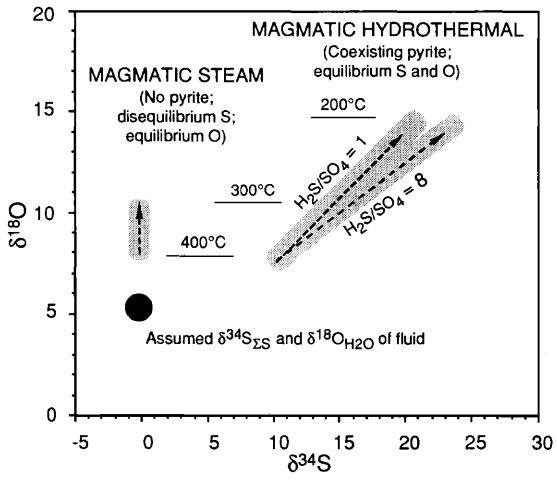

FIG. 5. Hypothetical $\delta^{34}S$ and $\delta^{18}O_{SO_4}$ values for magmatic steam and magmatic hydrothermal alunites formed from the same fluid (solid circle) over the temperature range 400° to 200°C and H_2S/SO_4 ratios of 1:1 and 1:8 for magmatic hydrothermal systems. See Rye et al. (1992) for details of calculations.

acid solutions ranges from days at 200° to minutes at 400°C (Table 1). These rates of equilibration are dependent upon total sulfur concentration of the fluids as well as their pH and temperature and are probably only approximate for magmatic systems. However, we can use this information to get a handle on the relative rates of ascent of magmatic fluids. Important for our purposes, isotope data sets which indicate lack of equilibrium between aqueous sulfur species in high-temperature systems imply very rapid flow of fluids. So much for principles, now let's look at magmatic fluid evolution as expressed in individual epithermal ore deposits.

Julcani: Vapor and Liquid Phase Magmatic Hydrothermal Fluid Evolution in the Epithermal Environment

Geologic framework

The Julcani district on the altiplano of Peru is an exceptional area for the study of silicic magmatism and related magmatic hydrothermal processes that result in epithermal mineralization. The important feature of this district is a remarkable, well-dated sequence of igneous and magmatic hydrothermal events that reached very shallow levels. The district has been the object of study for many years (Goodell and Petersen, 1974; Petersen et al., 1977; Drexler, 1982; Benavides, 1983; Noble and Silverman, 1984; Drexler and Munoz, 1985). The stable isotope story is part of a Ph.D. thesis by Jeff Deen supervised by John Drexler and Jim Munoz at the University of Colorado (Deen, 1990; Deen et al., 1987, 1988).

The Julcani district (Fig. 6) occurs in a late Miocene dome field that is built on a thick section of Paleozoic shales and carbonates. Four igneous events occurred over a time span of less than 500,000 years. The first two events, which produced the dome field, were the eruption of pyroclastics from a central vent and the emplacement of about 30 domes along regional fracture trends. The third igneous event was the emplacement of the Tentadora dacite dike. This dike was emplaced along a fracture trend most likely related to local stress produced by an underlying intrusion. The fourth important igneous event was the emplacement of the anhydrite-bearing Bulolo dike.

The earliest hydrothermal activity (Fig. 7) began after the emplacement of the Tentadora dike with the formation of fracture-controlled acid sulfate alteration zones. These zones have vuggy silica cores grading outward into quartz-alunite and quartz-kaolinite envelopes in a fashion typical of classical magmatic hydrothermal acid sulfate alteration zones (see discussion on the Summitville deposit). This alteration was overlapped in time and space by the formation of innumerable tourmaline-pyrite-quartz-altered breccia dikelets that extend radially over an area of 3 km^2. The highest concentration of these dikelets is in the center of the district. Six centers of mineralization then developed across the district in the reactivated regional fractures. Main-stage mineralization throughout the district was interrupted by the emplacement of the Bulolo dike. Late-stage mineralization then followed in the main-stage veins. The important point to keep in mind is that the main hydrothermal events were sandwiched in between the emplacement of the two, well-dated, dikes.

The ores at Julcani consist of Ag-Cu-Pb-W-Bi-Au-bearing mineral assemblages that occur as fracture fillings within the dacitic to rhyolitic domes and underlying tuffs. Mineralization reached within 200 to 300 m of the paleosurface. The ores are strongly zoned (Fig. 8) with a succession of pyrite-wolframite-gold-, enargite-, tetrahedrite-, galena-, and barite-dominant assemblages grading outward east and west from the central zone.

Temperatures and salinity of fluids

A summary of fluid temperature and salinity data is shown in Figure 9. The early vapor-phase acid sulfate

TABLE 1. Minimum Time Required to Attain 90 Percent Equilibrium between Sulfate and Sulfate at $\Sigma S = 0.01$ mole/Kg and pH = 2 (Ohmoto and Lasaga, 1982)

T°C	Time
400	0.8 hour
350	4.2 hours
300	15 hours
250	3 days
200	20 days

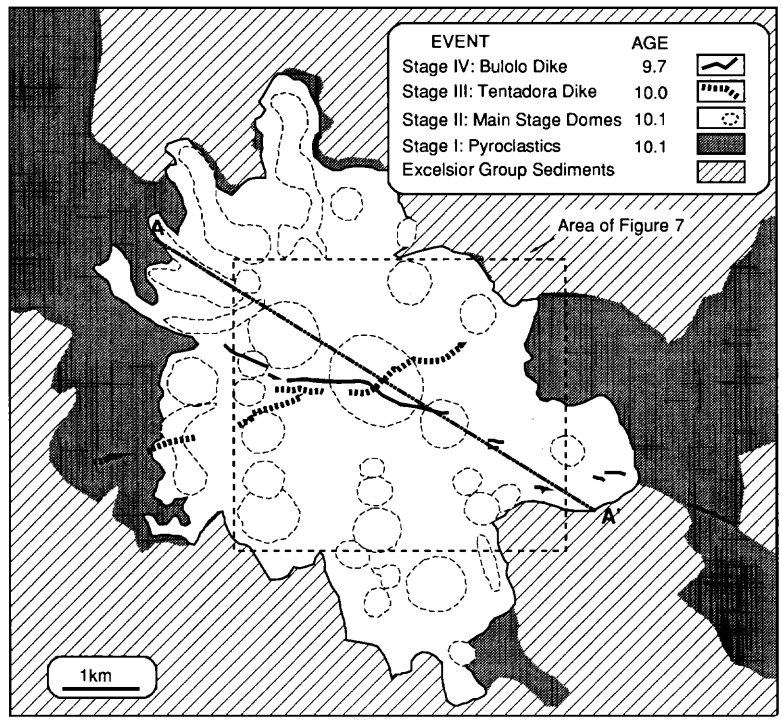

FIG. 6. Geology of the Julcani, Peru, dome field showing igneous stages and outline of individual domes. Modified from Deen (1990). Also shown is enlarged area of Figure 7 and line of section for Figure 8. Chronology (in Ma) is from K/Ar dating of Noble and Silberman (1984).

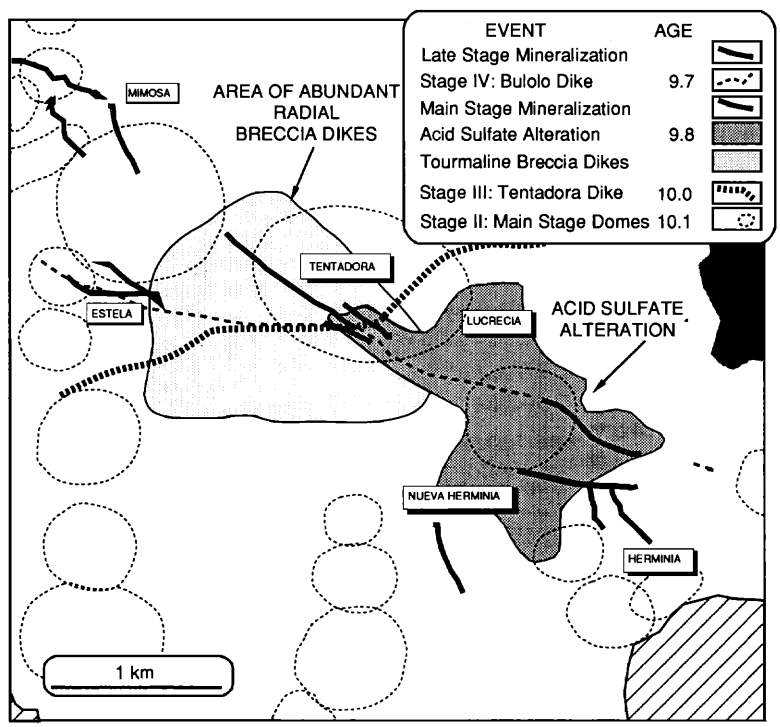

FIG. 7. Geology of the Julcani mining district showing pre- and postore dikes, outline of area of preore radial breccia dikes and acid sulfate alteration and location of major deposits. Modified from Deen (1990). Age is in Ma.

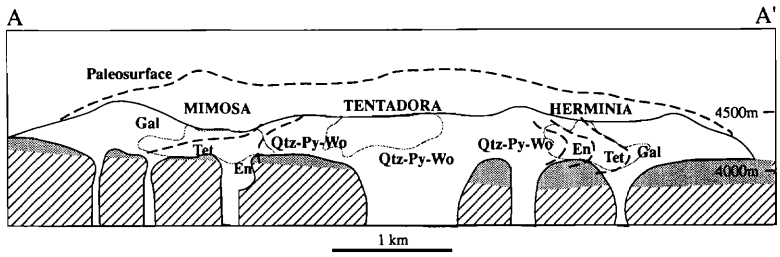

FIG. 8. Cross section of the Julcani mining district at the time of ore deposition showing projected location of orebodies and district-wide mineral zoning. Modified from Deen (1990). Patterns for the rock units are as in Figure 6. Abbreviations: En = enstatite, Gal = galena, Py = pyrite, Qtz = quartz, Tet = tetrahedrite, Wo = wolframite.

fluids had presumed low salinities and depositional temperatures averaging 260°C as determined by pyrite-alunite sulfur isotope thermometry. Fluids associated with the formation of the later tourmaline breccias were hypersaline with temperatures at least as high as 450°C. These hypersaline fluids, which were injected catastrophically, may be residual brines from the formation of the acid vapor plume or they may be related to the specific evolution of underlying magmas. The ore fluids had temperatures between 250° and 325°C and salinities between 7 and 20 wt percent. Even the late-stage fluids had high temperatures and salinities as high as 10 wt percent.

Stable isotope geochemistry

Figure 10 summarizes the sulfur isotope data on sulfur-bearing minerals from unaltered igneous rocks in the Julcani district, from the tourmaline breccias and acid sulfate alteration, and from the veins in the Herminia deposit. The sulfur isotope data on the preore Tentadora dike and the postore Bulolo dike indicate that the $\delta^{34}S$ value of bulk sulfur in the underlying magmas was about 5 to 6 per mil. Fluids in equilibrium with the parent magmas were shown by Jeff Deen (1990) to have been SO_2 rich. The $\delta^{34}S$ values for the hydrothermal sulfides are similar to those of the igneous sulfides whereas values for preore alunite and ore-stage barites are much larger than those for the igneous sulfate. Even though the fluids precipitated lots of sulfate, they were clearly H_2S rich with average H_2S/SO_4 ratios of about 5:1 as shown by the tie line in Figure 10 for a typical pyrite-alunite pair. These systematics indicate that the hydrothermal fluids were much more reducing than the primary magmatic fluids. The oxidation state of both preore and ore-stage hydrothermal fluids at Julcani appears to have been controlled by exchange with deep crystalline igneous rocks rather than by the primary magma.

The $\delta^{34}S$ values of alunite and coexisting pyrite from Julcani are typical of classical magmatic hydrothermal acid sulfate alteration zones (Rye et al., 1992). The data are consistent with the possibility that the sulfuric acid was derived from the disproportionation of SO_2 during the condensation of magmatic vapor at an average temperature of about 260°C. SO_2 begins to react with condensed water vapor in the plume to form sulfuric acid and H_2S at about 400°C according to the reaction: $4SO_2 + 4H_2O = 3H_2SO_4 + H_2S$ (Holland, 1965; Rye et al., 1992). Increasing amounts of H_2SO_4 and H_2S are produced as temperature decreases. The H_2SO_4 attacks the rocks to form acid sulfate alteration assemblages. H_2S reacts with iron in the system to form pyrite. Our concern here is the origin of the water.

The $\delta^{34}S$ and $\delta^{18}O$ isotope data on the SO_4 in alunites and calculated fluid compositions are shown in Figure 11. The narrow range of calculated $\delta^{18}O_{H_2O}$

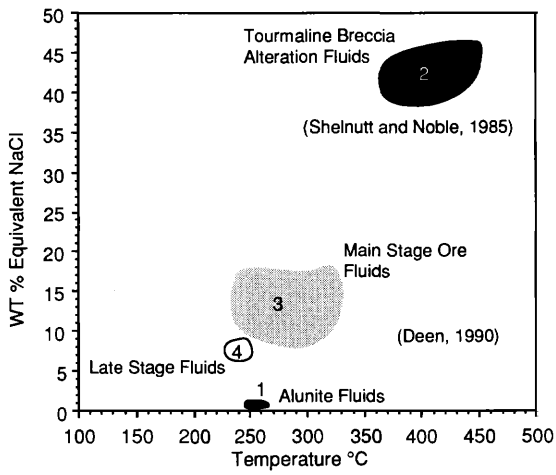

FIG. 9. Temperature and salinity data for preore and ore-stage hydrothermal fluids at Julcani. Numbers show position in paragenesis. Data on tourmaline breccia fluids (2) are from Shelnutt and Noble (1985); other data are from Deen (1990).

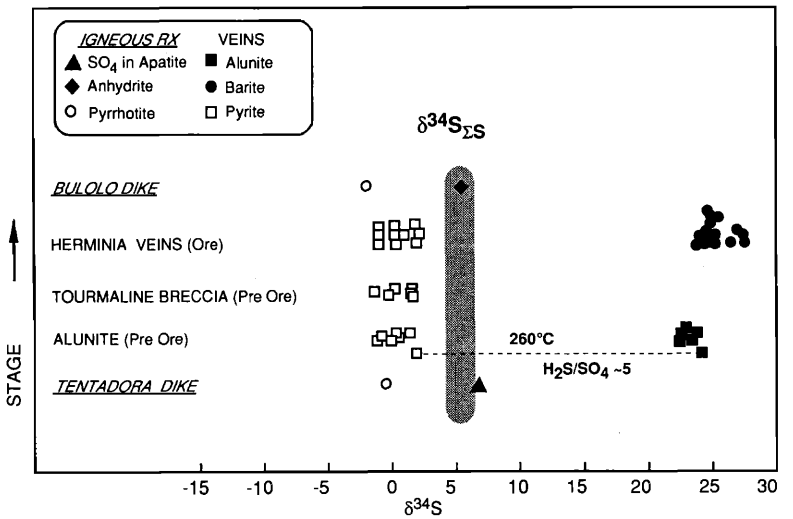

FIG. 10. $\delta^{34}S$ values of pyrite, alunite, and barite from veins (normal type) and SO_4 in apatite, anhydrite, and pyrrhotite from igneous rocks (underlined italics). Data are from Deen (1990). Tie line shows sulfur isotope temperature and H_2S/SO_4 of fluid for a typical alunite-pyrite pair. Shaded zone shows calculated $\delta^{34}S_{\Sigma S}$ for the system. Rx = rocks.

values for the fluids is consistent with the possibility that the disproportionation of SO_2 took place in nearly pure exchanged magmatic fluids. This possibility can be shown to be the case when we look at the δD values for alunite fluids (Fig. 12).

Figure 12 summarizes the hydrogen and oxygen isotope data of unaltered igneous biotites, preore alunites, and various fluids in the system. The calculated alunite fluids at Julcani have a rather narrow range of δD values averaging about −50 per mil. The δD of meteoric water during ore deposition, defined from analyses of fluids in late-stage minerals, is about −140 per mil. A beautiful mixing trend between evolved magmatic and unexchanged meteoric water is obvious from the data field based on Deen's (1990) analyses of fluid inclusions in many samples of vein minerals. These data correlate with the zoning shown previously in the cross section of the district. Clearly, mixing was a major cause of mineralization in the veins. What is interesting here is that the calculated hydrogen and oxygen isotope compositions of the alunite fluids and of the ore fluids are consistent with

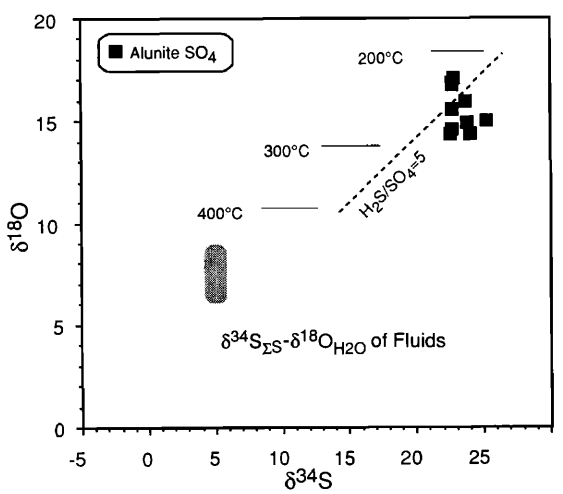

FIG. 11. $\delta^{34}S$ and $\delta^{18}O_{SO_4}$ values of alunite and calculated $\delta^{34}S_{\Sigma S}$ and $\delta^{18}O_{H_2O}$ values of fluid. Temperature and H_2S/SO_4 reference is described in caption for Figure 5. Data are from Deen (1990).

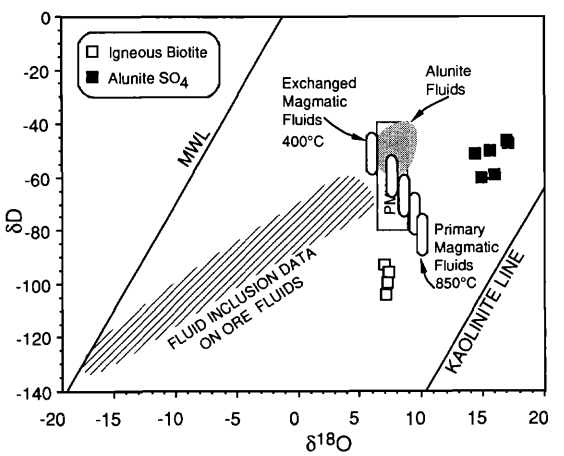

FIG. 12. δD and $\delta^{18}O$ values of preore alunite and igneous biotite and δD_{H_2O} and $\delta^{18}O_{H_2O}$ of fluids. Exchange track between primary magmatic fluids at 850°C and exchanged magmatic fluids calculated from biotite data as described in caption to Figure 2. Data are from Deen (1990). MWL = meteoric water line.

the composition of evolved magmatic fluids that reached the low-temperature end of the exchange track. The important lesson of Julcani is that, sandwiched in between igneous events, a magmatic vapor phase followed by hypersaline and saline liquid-phase fluids rose to very high levels and initially displaced the meteoric water in the host rocks. Although these fluids were of magmatic origin, exchange with deep crystalline rocks in a low water-rock environment apparently controlled their redox state and isotopic composition. The hydrothermal system at Julcani was so dominated by exchanged magmatic fluids that the district can be the standard by which the magmatic fluid contribution of all other epithermal systems can be evaluated.

Summitville, Colorado: The Lithostatic-Hydrostatic Transition and the Interfacing of Magmatic Hydrothermal Fluids with Meteroic Water

Geologic framework

At Summitville we can study a much smaller system than the one that produced the ores at Julcani. We can also study the Summitville system at deeper levels and better investigate the interfacing of magmatic and meteoric water. Roger Stoffregen conducted pioneering studies in the area (Stoffregen, 1987) and he, Phil Bethke, and I have continued to work there (Rye et al., 1990). The deposit occurs on the margin of the Platoro-Summitville caldera complex in the San Juan volcanic field. It is a classic example of epithermal Cu-Au-Ag mineralization associated with acid sulfate alteration in a relatively near surface environment.

The Summitville gold deposit lies within the coarsely porphyritic quartz latite of the South Mountain volcanic dome shown in Figure 13 as reconstructed during mineralization. K/Ar dating of alunite and the enclosing South Mountain porphyry indicates that emplacement of the dome and mineralization were nearly coincident at 22.5 Ma. Mineralization and alteration occur in fault-controlled, subvertical, acid sulfate alteration zones within the South Mountain porphyry. Gold mineralization occurs within a thousand feet of the present surface, but drilling has shown that the hydrothermal system extended over a vertical range of at least 4,500 ft. A probably genetically related quartz monzonite porphyry intrusion with Cu anomalies, phyllic alteration, and a stockwork zone with pyrite and minor quartz fillings occurs beneath the district at elevations below 10,000 ft. Peter Vikre (writ. commun., 1992) observed in a reconnaissance study several years ago that some fluid inclusions in the deep quartz fillings have salinities of over 40 wt percent NaCl equiv.

Figure 14 shows a typical small acid sulfate alteration zone. The center of the zone consists of vuggy silica core in which the large sanidine phenocrysts have been completely removed. Adjacent to the vuggy silica the feldspars have been replaced by pink alunite in a zone about 25 cm thick. Farther out the feldspars have been replaced by white kaolinite. Most gold occurs in the vuggy silica with later covellite, enargite, luzonite, and chalcopyrite. These zones can range up to 70 m across and be enclosed by up to 30 m of intense quartz-alunite alteration and extend to depths of up to 200 m (Stoffregen, 1987).

Stable isotope geochemistry

The overall sulfur isotope systematics of the Summitville system are very similar to those at Julcani (Fig. 15). The $\delta^{34}S$ values of the bulk sulfur in the

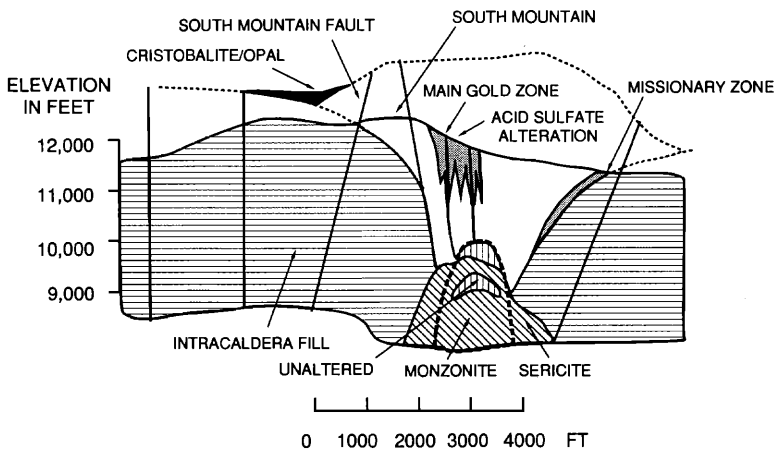

FIG. 13. Schematic cross section of the Summitville district showing reconstructed geology at the time of mineralization. Modified from Steven and Ratte (1960) and Gray and Coolbaugh (in prep.).

FIG. 14. A typical small acid sulfate alteration zone at Summitville. The center of the zone near the hammer consists of vuggy silica core in which the large sanidine phenocrysts have been completely removed. Adjacent to the vuggy silica is a 25-cm-thick quartz-alunite zone where the feldspars have been replaced by pink alunite. This zone is in turn enveloped by a quartz-kaolinite zone where the feldspars at the left edge of the photograph have been replaced by white kaolinite. Gold occurs in the vuggy silica with later covellite, enargite, luzonite, and chalcopyrite. The zoning reflects the progressive neutralization of the condensed magmatic vapor fluids through reaction with wall rock and mixing with surrounding meteoric waters.

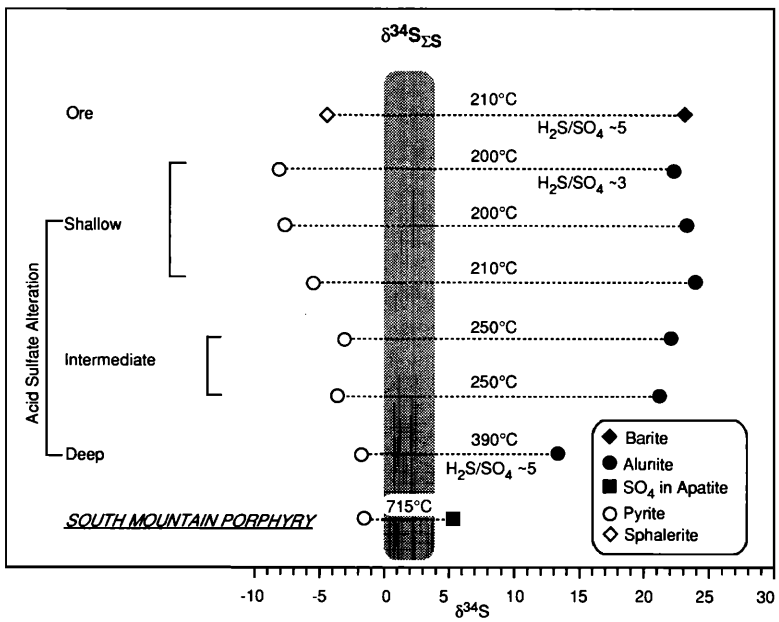

FIG. 15. $\delta^{34}S$ values and calculated temperatures of coexisting sulfide and sulfate minerals from South Mountain porphyry, various levels of acid sulfate alteration, and main-stage ore. Tie lines show temperatures and H_2S/SO_4 of coexisting samples. Rectangle shows $\delta^{34}S_{\Sigma S}$ of the systems. Data are from Rye et al. (1990).

system must have been between the values for sulfate and sulfide in the igneous rocks and was most likely between 0 and 4 per mil. Using this range of $\delta^{34}S$ values for the bulk sulfur as a fulcrum, the $\delta^{34}S$ data for coexisting vein sulfides and sulfates require that the hydrothermal fluids were sulfide dominant. The Summitville hydrothermal fluids, like those at Julcani, most likely followed a reducing path after exsolution from oxidizing magma. The temperatures based on $\delta^{34}S$ values of coexisting vein sulfate and sulfide minerals vary systematically with elevation in the deposit and are in excellent agreement with those observed for filling temperatures of secondary fluid inclusions in quartz phenocrysts in the South Mountain porphyry (Bruha and Noble, 1983).

When the sulfur isotope temperatures are plotted as a function of reconstructed elevation (Fig. 16), the shallowest samples fall close to the hydrostatic boiling curve for the system. The deepest sample, however, falls close to the lithostatic boiling curve. This suggests that the transition from lithostatic to hydrostatic conditions or the brittle-ductile transition occurred between approximately 9,000- and 10,000-ft present elevation, about 4,500 ft below the paleosurface. Because this elevation is the deepest occurrence of alunite, it probably also coincides with the base of the vapor plume.

The sulfur and oxygen isotope data on SO_4 in alunites at Summitville (Fig. 17) show a much larger range than that observed at Julcani. This larger range is partly due to the fact that alunite formation took place over a larger temperature interval at Summitville. However, the larger range of ^{18}O values for the fluids suggests that the disproportionation of some SO_2 occurred in fluids that had a small meteoric water component. This conclusion is further supported by data in Figure 18 in which alunites with the lowest ^{18}O values also have the lowest δD values.

Although the data show more scatter, the hydrogen and oxygen isotope data on the minerals and

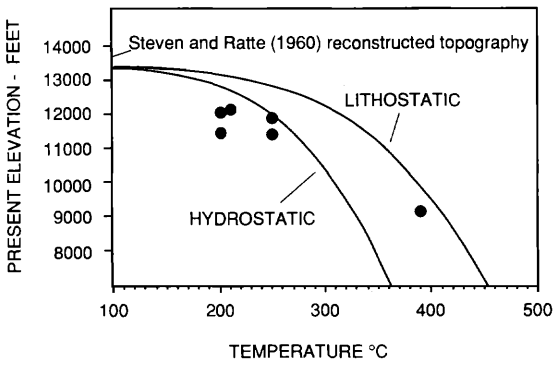

FIG. 16. Alunite-pyrite sulfur isotope temperatures versus present elevation and relation to lithostatic and hydrostatic boiling curves (Rye et al., 1990).

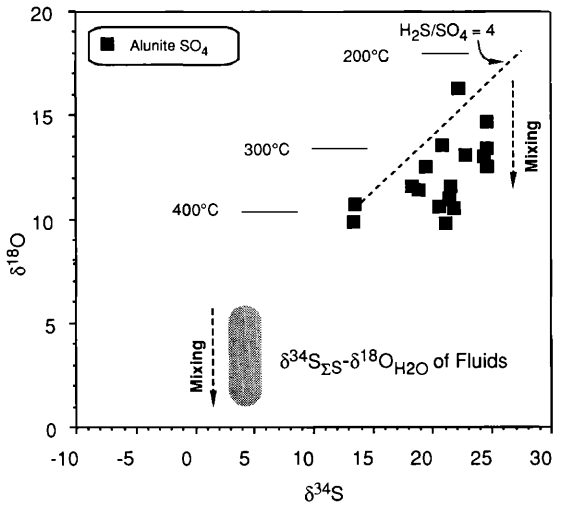

FIG. 17. $\delta^{34}S$ and $\delta^{18}O_{SO_4}$ values of alunite and calculated $\delta^{34}S_{\Sigma S}$ and $\delta^{18}O_{H_2O}$ of fluid. Also shown is the possible mixing trend. The temperature and H_2S/SO_4 reference is described in caption for Figure 5. Data are from Rye et al. (1990).

fluids at Summitville are generally similar to those at Julcani (Fig. 12). The δD values of the alunite fluids range from about −30 to −70 per mil. The greater scatter in the alunite fluid isotope data at Summitville reflects the smaller size of the magmatic vapor plume and its correspondingly greater susceptibility to isotope variations due to mixing with local meteoric water, water-rock exchange, and boiling. The tendency for kaolinite and alunite fluids to have dis-

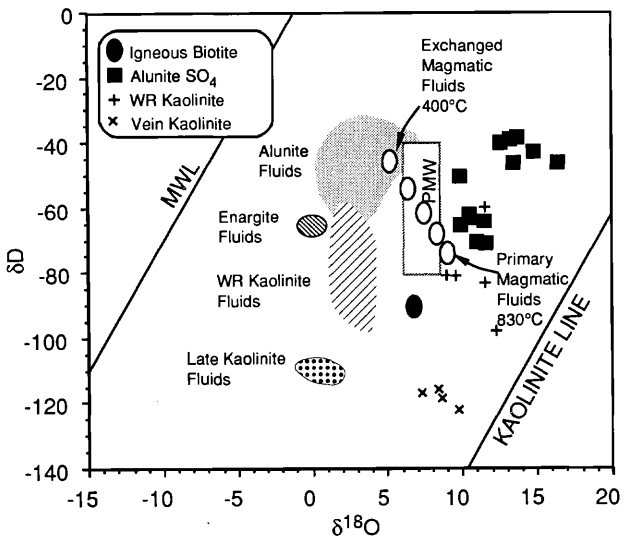

FIG. 18. δD and $\delta^{18}O$ values of preore alunite, wall-rock kaolinite, vein kaolinite, and igneous biotite and δD_{H_2O} and $\delta^{18}O_{H_2O}$ of fluids (shaded patterns). Exchange track (open symbols) calculated from biotite data as described in caption for Figure 2. Data are from Rye et al. (1990) and Rye (unpub. data). MWL = meteoric water line, PMW = primary magmatic water box.

tinctly different δD values but the same $\delta^{18}O$ values suggests that the vapor plume essentially displaced exchanged meteoric water in the country rock around the individual veins. Kaolinite in the wall rock formed as a result of mixing with meteoric water and neutralization of acid condensates from the acid vapor plume. Kaolinite in the late veins has lower δD values, indicating formation from predominately meteoric water. The δD values of enargite fluids indicate that the main-stage sulfides also formed from exchanged liquid phase magmatic fluids. Magmatic fluid evolution at Summitville appears to have been very similar to that at Julcani where evolved magmatic vapor phase and later ore-bearing liquid phase fluids displaced meteoric water at high levels. The isotopic and chemical characteristics of these magmatic fluids were also determined largely by exchange with deep crystalline rocks. The gift from Summitville is the evidence indicating that the base of the early vapor plume was near the hydrostatic to lithostatic pressure transition in the rocks.

Marysvale Alunite Ridge-Deer Trail Mountain, Utah: The Type Locality for Magmatic Steam Alunite

Geologic framework

Alunite Ridge near Marysvale, Utah, is the site of some remarkable alunite deposits. Skip Cunningham (Cunningham et al., 1984) introduced me to this area and Skip, Phil Bethke, and I continue to work there. The area actually contains two 14 Ma hydrothermal centers, Alunite Ridge in the west and Deer Trail Mountain in the east (Fig. 19). Both centers developed in a volcanic sequence that overlies Mesozoic and Paleozoic sediments at the edge of the Basin and Range province. Each center occurs in areas of radial and concentric fracturing and central uplift which were almost certainly related to the forceful injection of two unexposed cupolas. At Alunite Ridge the cupola was injected so forcefully that the volcanic rocks are steeply dipping in the vicinity of the veins. Alunite Ridge contains numerous veins of alunite with virtually no coeval quartz, kaolinite, or pyrite. The alteration at Deer Trail Mountain consists of quartz + pyrite veins surrounded by altered volcanic rocks. A number of metallic mineral deposits occur in the sediments in an annular ring surrounding the Alunite Ridge and Deer Trail Mountain complex. One of these deposits occurring in limestones near the eastern end of the district is the previously investigated Deer Trail mine (Beaty et al., 1986).

The cross section (Fig. 20) shows the presumed relationship of the Alunite Ridge and Deer Trail Mountain hydrothermal centers and the Deer Trail mine to hidden stocks at depth. The different fluid evolution at the two centers probably reflects differences in the degree of doming and corresponding openness of the rocks and depth to underlying intrusions.

Nearly pure alunite occurs at Alunite Ridge as open-space fillings in extensional fractures that are as much as 20 m wide and 100 m deep. These are among the largest, purest, most coarsely crystalline veins of alunite in the world. They contain only a minute amount of fine hematite and quartz. Much of the rock adjacent to veins is unaltered.

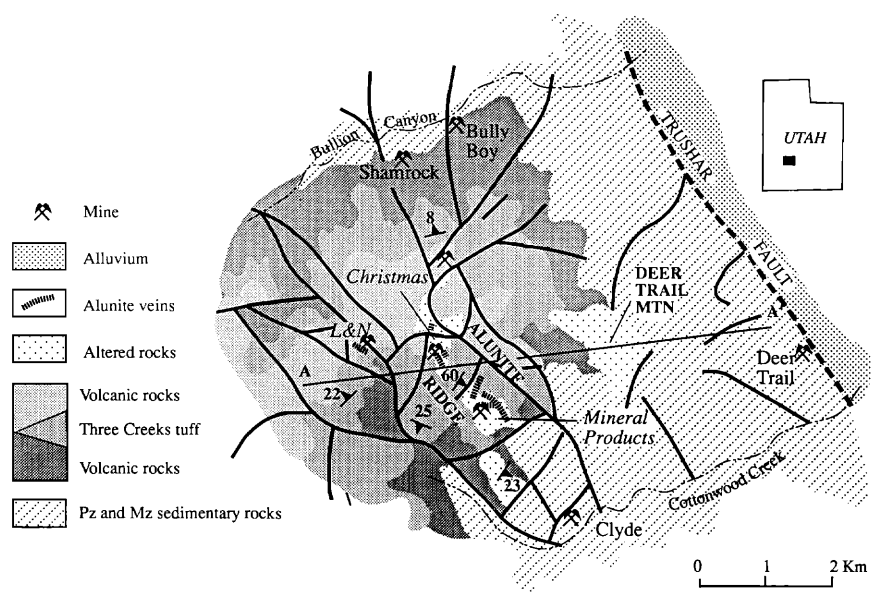

FIG. 19. Geology of the Deer Trail Mountain-Alunite Ridge area showing line of section for Figure 20. Modified from Cunningham et al. (1984). Mz = Mesozoic, Pz = Paleozoic.

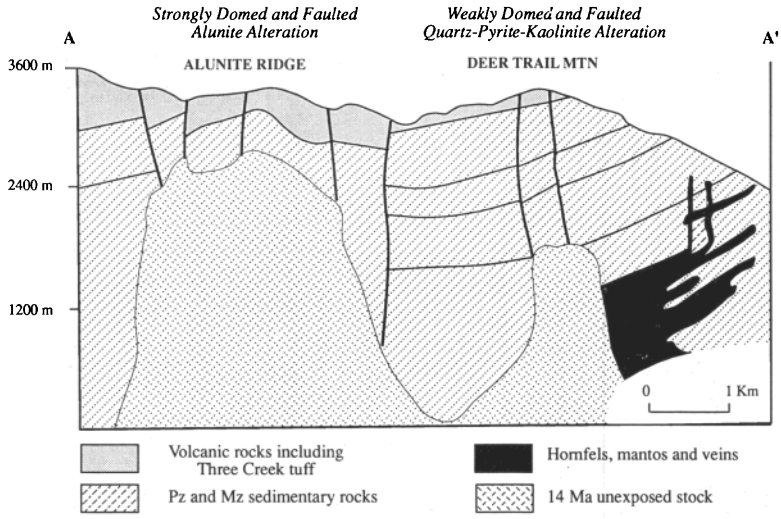

FIG. 20. Cross section of Deer Trail Mountain-Alunite Ridge area showing alteration, postulated copulas underneath each area, and Deer Trail mineralization. Modified from Beaty et al. (1986). Mz = Mesozoic, Pz = Paleozoic.

The alunites are beautifully banded (Fig. 21). I suspect that each band in the alunite reflects an event in the history of an underlying magma, and as such, this sample shows the episodic nature of magmatic processes. Inclusion fluids in the alunite are vapor rich indicating formation from low-density vapor. This type of alunite has been observed at Alunite Ridge and elsewhere only in open tensional fractures and breccias, an environment that indicates a depressuring of the hydrothermal system.

Stable isotope geochemistry

Figure 22 shows the hydrogen and oxygen isotope composition of alunites at Alunite Ridge and their calculated fluid compositions along with the composition of fluids measured directly from inclusion fluids in minerals from the Deer Trail mine. The hydrogen and oxygen isotope geochemistry of the Alunite Ridge-Deer Trail Mountain system is similar to that at Julcani (Fig. 12). The hydrogen and oxygen isotope values of the Deer Trail fluids show a good correlation that also relates to their salinity. Clearly two fluids were involved in the formation of the Deer Trail manto deposit—a dilute meteoric water with a δD of about -125 per mil and a saline, probably ex-

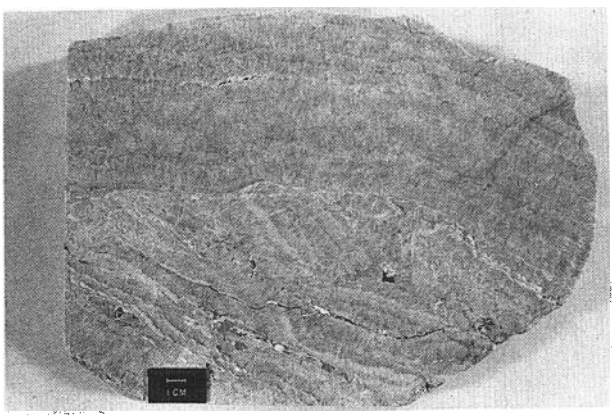

FIG. 21. Polished slab of magmatic steam alunite from Alunite Ridge showing banding (Cunningham et al., 1984). The broken rotated layers in the lower portion of this sample may indicate that deposition was concurrent with structural deformation. Each band probably represents a magmatic event.

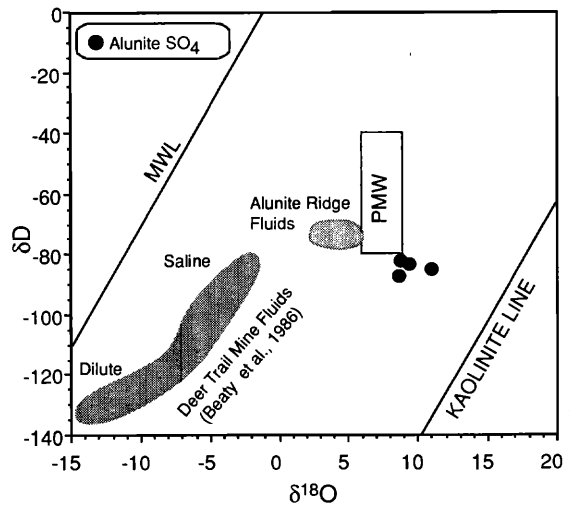

FIG. 22. δD and $\delta^{18}O_{SO_4}$ values of Alunite Ridge alunite and δD_{H_2O} and $\delta^{18}O_{H_2O}$ of fluids. Data from Rye et al. (1992). Also shown is composition field of Deer Trail mine fluids from analyses of inclusion fluids (Beaty et al., 1986). MWL = meteoric water line, PMW = primary magmatic water box.

changed magmatic water with a δD no lower than −75 per mil. The average δD value of −70 per mil for fluids at Alunite Ridge is consistent with a magmatic origin.

The sulfur and oxygen isotope data on sulfate in alunite and calculated fluid compositions at Alunite Ridge are very different from those at Julcani and Summitville (Fig. 23). The $\delta^{34}S$ values of the alunite are very tightly clustered near 0 per mil which is the value for the bulk sulfur in the magmatic system as indicated by the sulfur isotope data on minerals in the Deer Trail deposit. The sulfur isotope values in alunite are characterized by complete disequilibrium which indicates that disproportionation of SO_2 did not occur in the fluids. This isotopic disequilibrium in the alunites indicates that the fluids ascended much faster than the rate of sulfur isotope exchange between aqueous sulfur species. If the rates of sulfur isotope exchange shown in Table 1 for low pH fluids are relevant, the fluids traveled from their source to site of deposition in less than a few minutes.

The alunite fluids were probably SO_2 rich, much as are volcanic gases that are released at high temperatures and low pressures. SO_2 is produced from H_2S during depressuring of magmatic fluids by the reaction: $2H_2O + H_2S = SO_2 + 3H_2$ (Gerlach, 1993). This reaction also produces H_2 which we have observed in reconnaissance gas studies of the inclusion fluids of the Alunite Ridge samples. Alunite probably formed as the magmatic steam decompressed in the open spaces of the veins. Exactly how SO_2 was oxidized to SO_4 to form alunite is not understood, but it is likely

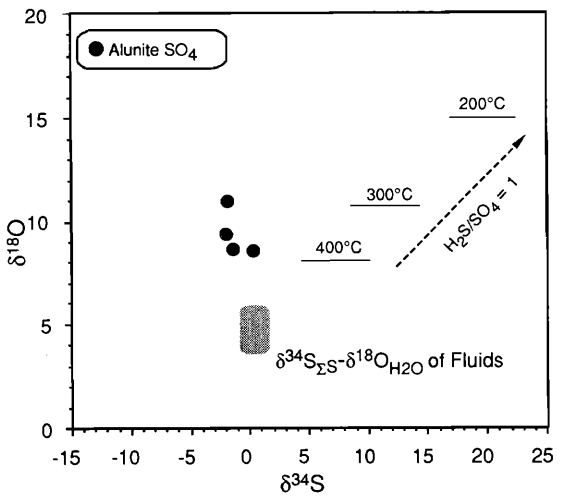

FIG. 23. $\delta^{34}S$ and $\delta^{18}O_{SO_4}$ values of alunite and calculated $\delta^{34}S_{\Sigma S}$ and $\delta^{18}O_{H_2O}$ of fluids shown against temperature and H_2S/SO_4 reference described in caption for Figure 5. Data are from Rye et al. (1992).

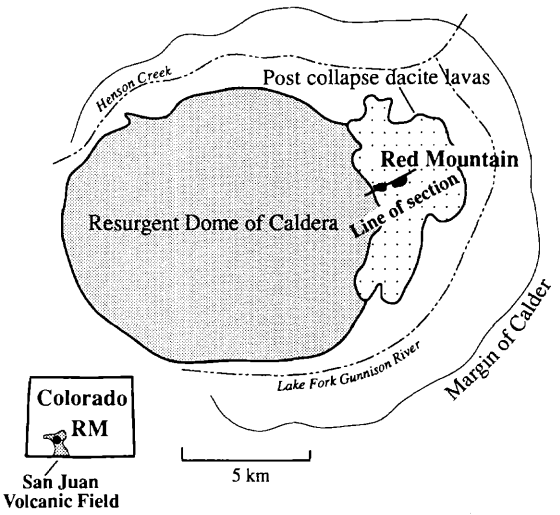

FIG. 24. Generalized geology of the Red Mountain Area, Lake City, Colorado, showing resurgent dome of Lake City caldera, post-collapse dacite lavas and porphyry intrusions, and line of section for Figure 25 (Bove and Hon, 1990).

that loss of hydrogen is involved. Our study of these alunites is continuing and they have much to teach us about the evolution of magmatic fluids. In order to better understand the fundamental difference between magmatic steam alunites at Alunite Ridge and magmatic hydrothermal alunites at Julcani and Summitville we need to turn to our study at Red Mountain.

Red Mountain, Lake City, Colorado: The Rate of Flow of Vapor-Phase Magmatic Hydrothermal Fluids

Geologic and mineralogic framework

Red Mountain near Lake City, Colorado, is the site of one of the largest replacement alunite deposits in the western United States with about 70 million tons of alunite. Dana Bove, my colleague at the U. S. Geological Survey, is responsible for important detailed work on these alunites and underlying alteration assemblages as part of a masters thesis at the University of Colorado (Bove, 1988; Bove et al., 1990). The deposit occurs in a complex of high K dacite intrusions and flows on the eastern ring fracture zone of the strongly resurgent 23 Ma Lake City caldera that lies in the San Juan volcanic field (Fig. 24). K/Ar dating indicates that alunite alteration was essentially synchronous with emplacement of the host rocks near the conclusion of the caldera cycle.

The deposit consists of two roughly conical centers with roots extending more than 1,000 ft beneath the surface in which alunite makes up more than 30 percent of the rock (Fig. 25). Alunite-quartz-pyrite rock

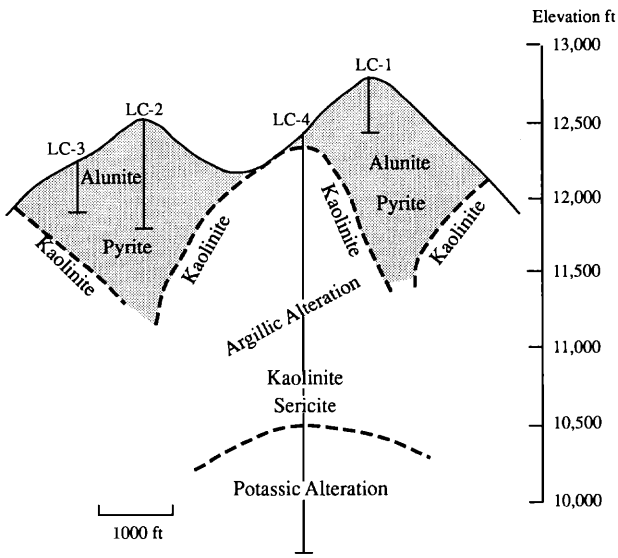

FIG. 25. Cross section of hydrothermally altered area at Red Mountain, Lake City, Colorado, showing profile of Red Mountain and adjacent lower peak and location of drill holes (Bove and Hon, 1990).

changes outward into argillized and propylitized dacitic volcanics and downward through argillic, sericitic, and potassic alteration zones in a fashion typical of classical porphyry-type alteration. A 2,500-ft exploratory drill hole established that the deposit overlies a weak molybdenite porphyry-type system with slightly elevated F/Cl ratios in sericites and secondary biotites. Several additional drill holes have permitted sampling of the alunite, thus supplementing samples collected at the surface.

Bove recognized four major stages of alunite (Fig. 26). Stages 1 and 2 are magmatic hydrothermal alunites such as occur at Julcani and Summitville. They comprise over 95 percent of the alunite at Red Mountain. Stages 3 and 4 are magmatic steam alunites that occur in brecciated rock and tension fractures such as we saw at Alunite Ridge. Hydrothermal brecciation is widespread at Red Mountain and a major period of brecciation prior to stage 3 alunite deposition can be tentatively correlated with the formation of secondary biotite in the porphyry system at depth.

Stable isotope geochemistry

The sulfur isotope systematics at Red Mountain are different in several informative respects from any deposit that we have investigated (Fig. 27). Primary magmatic fluids were probably reduced and the near 0 per mil $\delta^{34}S$ value of the pyrrhotite in the dacites and of pyrite in the porphyry alteration probably represents the composition of the bulk sulfur in the underlying magmas. The total range of $\delta^{34}S$ values for the four stages of alunite as shown in the solid symbols is a remarkable 30 per mil from about −3 to 27 per mil. The stage 1 and 2 magmatic hydrothermal alunites have classical equilibrium sulfur isotope systematics as shown by the tie lines. Stage 1 alunite fluids had an H_2S/SO_4 ratio of about 1 which is the lowest that we have seen for a magmatic hydrothermal system. The magmatic steam alunites have disequilibrium sulfur isotope values close to the bulk sulfur in the system and almost certainly formed from SO_2-rich fluids. In contrast to Julcani and Summitville, hydrothermal fluids at Red Mountain were probably more oxidizing than the primary magmatic fluids. A great deal of hydrothermal brecciation occurred at Red Mountain and stage 4 veins occur in tensional fractures. The SO_2-rich nature of the vapor fluids was likely related to the frequent catastrophic depressuring of the hydrothermal system.

The sulfur and oxygen isotope data on sulfate in the

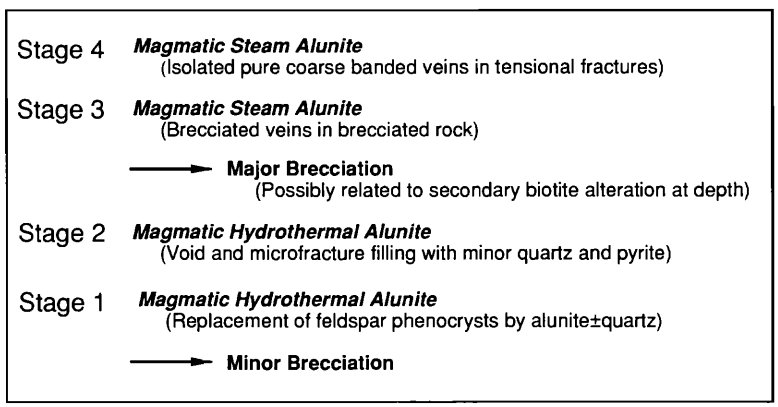

FIG. 26. Paragenesis of Red Mountain, Lake City, Colorado, alunites (Bove, 1988).

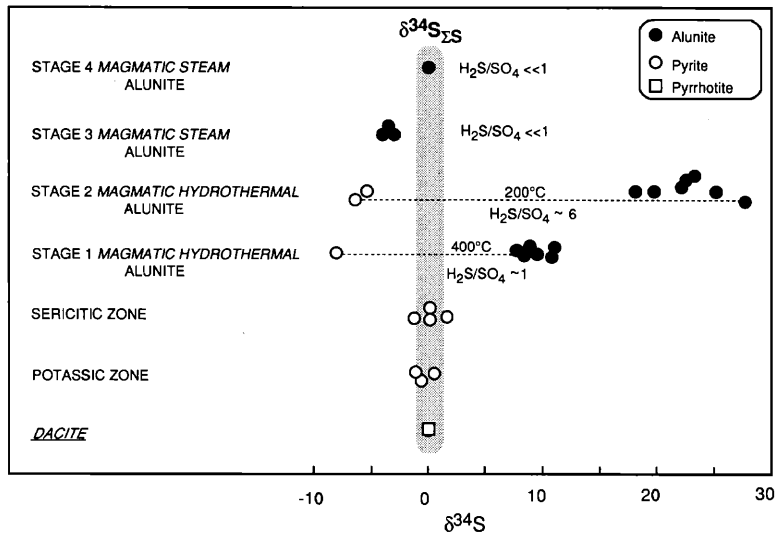

FIG. 27. $\delta^{34}S$ values of pyrite in different zones of porphyry alteration, coexisting pyrite and alunite from various stages of acid sulfate alteration, and pyrrhotite in cogenetic dacites. Tie lines show temperatures and H_2S/SO_4 of coexisting samples. Rectangle shows $\delta^{34}S_{\Sigma S}$ of the systems. Data are from Bove et al. (1990) and Rye (unpub. data).

alunites (Fig. 28) are similar to the hypothetical ones for magmatic hydrothermal and magmatic steam alunites shown in Figure 6. Even though the alunite compositions are all over the diagram, the calculated fluids have a narrow range of values. The point here is that a single fluid was probably responsible for all four stages of alunite. The huge differences in stable isotope geochemistry between the different types of alunite at Red Mountain are best interpreted to reflect the differences in the pressure at which the fluids were released from their source and in the rate at which they ascended.

The hydrogen and oxygen isotope geochemistry of the fluids (Fig. 29) is very similar to that at Summitville and Julcani. The alunite fluid compositions have

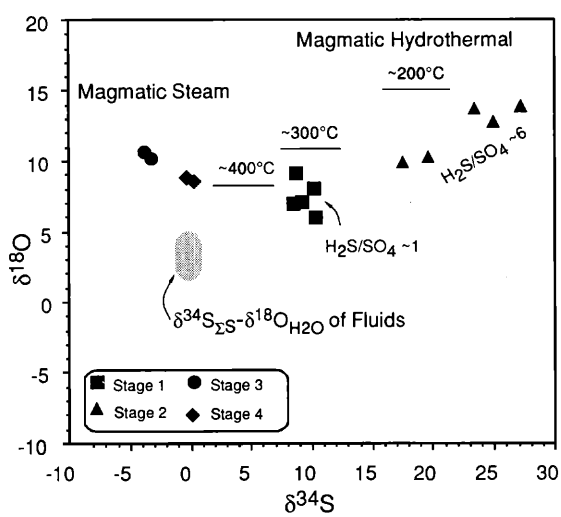

FIG. 28. $\delta^{34}S$ and $\delta^{18}O_{SO_4}$ values of various stages of alunite and calculated $\delta^{34}S_{\Sigma S}$ and $\delta^{18}O_{H_2O}$ of fluid. Temperature and H_2S/SO_4 reference is described in caption for Figure 5. Data are from Bove et al. (1990).

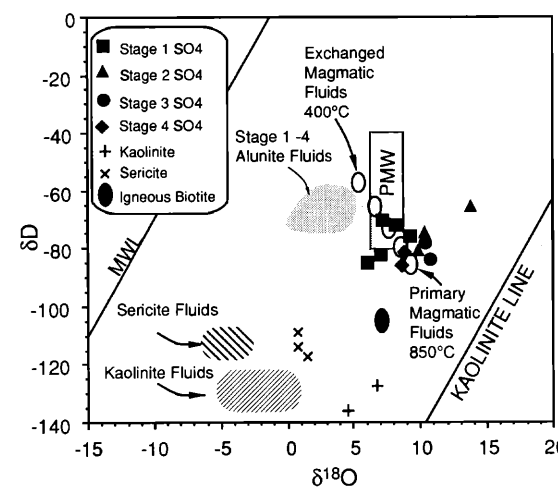

FIG. 29. δD and $\delta^{18}O$ values of igneous biotite from cogenetic dacite, various stages of alunite, kaolinite, and sericite, and δD_{H_2O} and $\delta^{18}O_{H_2O}$ of fluids (shaded patterns). Exchange track (open symbols) calculated from biotite data as described in caption for Figure 2. Data are from Bove et al. (1990) and Rye (unpub. data). MWL = meteoric water line, PMW = primary magmatic water box.

a narrow range with an average δD of -50 per mil and are distinctly different than those for kaolinite fluids at the margin of the deposit and for the sericite fluids from the porphyry alteration at depth. Clearly the alunites formed from predominantly exchanged magmatic fluids with little meteoric water entrainment. In common with Julcani and Summitville, all alunite fluids, including those for magmatic steam alunites, have isotopic compositions that indicate equilibration with deep crystalline rocks. There is a lot of alunite at Red Mountain so the accumulative size of the magmatic vapor plume that produced it was substantial. Almost certainly this plume was episodic rather than continuous. The important contribution of our study at Red Mountain is that large differences in the rate of flow of fluids in the plume can be detected from the stable isotope geochemistry of the alunites.

Providencia, Mexico: The Rate of Flow of Liquid-Phase Magmatic Hydrothermal Fluids

Geologic and mineralogic framework

Having made these remarks about rates of flow of magmatic vapor-phase fluids, I would like to comment on the rate of flow of ore-bearing magmatic saline liquid-phase fluids. For this discussion I want to turn to some of the relevant observations that Sam Sawkins and I made as young graduate students nearly 30 years ago at Providencia (Sawkins, 1964; Rye, 1966). The Providencia district consists of conformable pipelike bodies of Pb-Zn sulfide ore that occur in steeply dipping Mesozoic limestones on the south limb of an anticline that has been intruded by a granodiorite stock (Fig. 30). There are about 30 pipes in the area which produced over 10 million tons of sulfide ore. These pipes were mined to depths of over 1,000 m. At 40 Ma the deposits are the oldest that I have discussed today and they are probably also the deepest.

Magnetite-quartz veinlets up to 5 cm thick occur in the uppermost part of the granodiorite stock. These veinlets formed above 400°C from high-salinity fluids that produced fluid inclusions with multiple daughter minerals. Although we do not know the time of emplacement of these saline fluids, our experience at Julcani would lead us to look for evidence for a counterpart magmatic vapor plume. The ores at Providencia were very vuggy and much open space in the host rocks appeared to have been present prior to mineralization. I believe that this open space was created from the dissolution of limestone by an early magmatic vapor plume such as that which produced the vuggy silica in volcanic host rocks at Julcani and Summitville.

Temperature and salinity of fluids

Sawkins determined that the average temperature of mineralization at Providencia declined continually over a range of nearly 175°C (Fig. 31). Most important, Sawkins could not detect temperature gradients in the main-stage mineralization over a vertical distance of 1,000 m in the pipes. This lack of temperature gradients argues for rapid ascent of the fluids. Sam also discovered that the salinity of the hydrothermal fluids varied from about 10 to 40 wt percent. Amazingly, these salinity variations were highly erratic and were independent of all other parameters in the hydrothermal system, including mineralogy, paragenesis, composition of individual minerals, temperature, and isotopic composition of the fluids. The

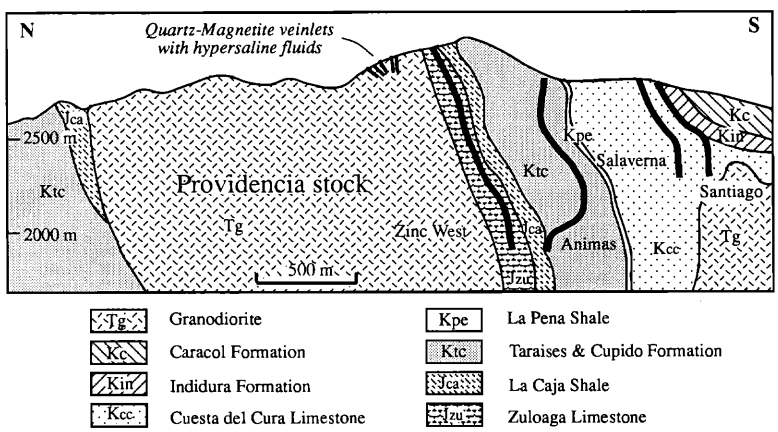

FIG. 30. Northeast-southwest cross section of the Providencia mining district showing location of orebodies in limestones and quartz-magnetite veinlets in the granodiorite stock. Modified from Sawkins (1964).

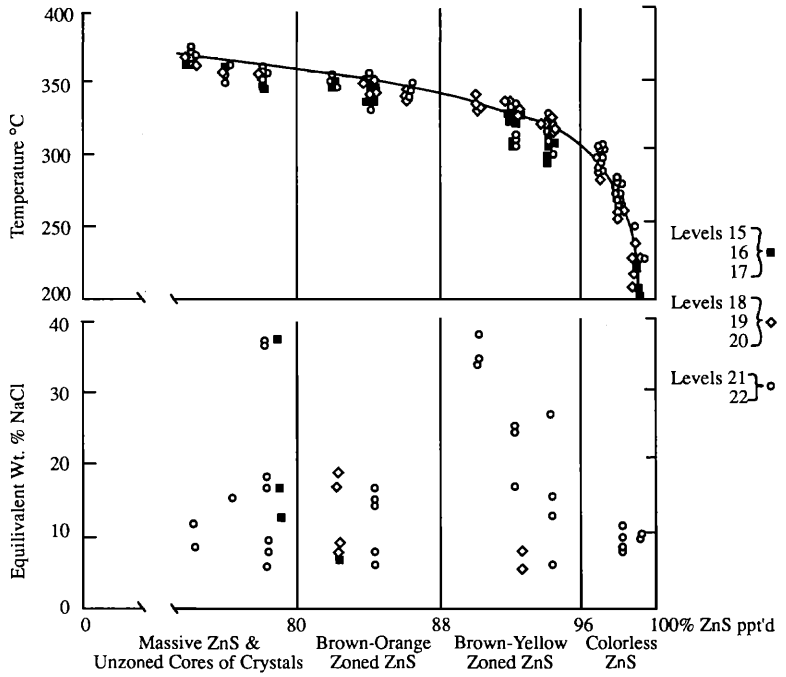

FIG. 31. Filling temperatures and salinities in sphalerite from the Animas orebody at Providencia (Sawkins, 1964).

cause of these salinity variations is still a matter of conjecture, but they are consistent with variations that might develop in residual fluids at the base of a vapor plume near the brittle-ductile transition.

Stable isotope geochemistry

The δD and $\delta^{18}O$ values of the water in the fluids were nearly constant throughout main-stage mineralization and were independent of temperature and salinity variations (Fig. 32). These fluid compositions were way out of isotopic equilibrium with the limestone host rocks. Although I could not obtain information on unaltered cogenetic igneous rocks at Providencia, the simplest interpretation of its fluid history is that both the chemical and isotopic compositions of the ore fluids were buffered by exchange with crystalline rocks at depth. The lack of significant exchange of the ore fluids with wall rocks at high levels largely reflects the high rate at which the fluids flowed up the flue.

Model for Magmatic Fluid Evolution in the Epithermal Environment

Early vapor-phase fluid stage

Returning to the cartoon (Fig. 1) shown at the beginning of the talk, we can now summarize the fundamental processes that occur during the evolution of magmatic fluids in the epithermal environment. This cartoon represents the earliest stage of a magmatic hydrothermal system. It is obviously oversimplified as many systems are complicated by multiple magmatic events. Also not all magmatic fluid systems, such as those that underlie large meteoric water hydrothermal systems, undergo the evolution shown here. In such systems the magmatic contribution to

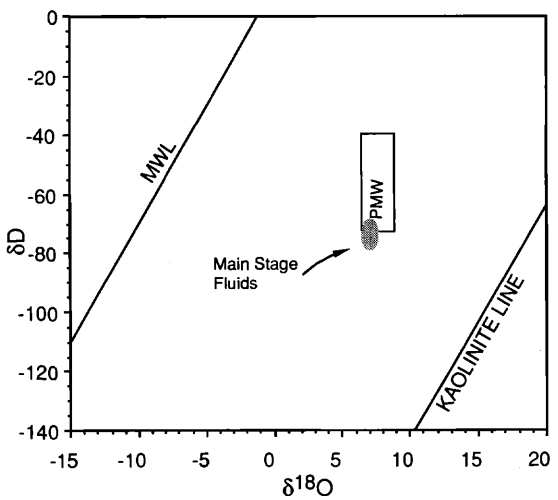

FIG. 32. δD_{H_2O} and $\delta^{18}O_{H_2O}$ values of Providencia main-stage ore fluids. Composition field from Rye (1966). MWL = meteoric water line, PMW = primary magmatic water box.

the epithermal environment will be largely limited to heat and gases from the magma.

The first manifestation of a magmatic fluid hydrothermal system is frequently the formation of an acid vapor plume in the shallow levels of the system as we saw at Julcani and Summitville. This vapor plume will have its roots near the lithostatic to hydrostatic transition in the rocks as we saw at Summitville. The plume will likely wax and wane and flow in pulses that reflect the episodic nature of magmatic processes as we saw at Marysvale and Red Mountain. Plumes whose fluids ascend relatively slowly will have high H_2S/SO_2 ratios and isotopic compositions buffered by exchange with deep crystalline rocks. When the vapor in the plume condenses, SO_2 will disproportionate and the resulting low pH fluids will attack the rocks, creating a chimney of permeability. In volcanic environments such as Julcani and Summitville this permeable zone will comprise vuggy silica surrounded by quartz-alunite and quartz-kaolinite envelopes. In limestone environments the permeable zones will be large cavities as at Providencia. However, in systems that are suddenly depressured, an SO_2-rich magmatic vapor may ascend rapidly and expand in open spaces producing almost pure banded alunite with little wall-rock alteration such as that at Marysvale. Both types of plumes may form above porphyry-type systems such as that at Red Mountain, Lake City. Very little meteoric fluid is entrained in these magmatic vapor plumes as they effectively displace meteoric water in the country rock. However, when the vapor condenses, it will eventually mix with the meteoric water to form kaolinite. These acid vapor plumes are an important part of the evolution of a magmatic hydrothermal system. They may cause salinity variations in ore fluids and be important in the formation of early hypersaline brines in the system. They play an important role in the neutralization of magmatic fluids and in the process form shallow permeability zones that help give the underlying liquid-phase fluids in the system a clear shot to the hydrostatic environment at high levels.

Main (ore-bearing) liquid-phase fluid stage

As magmatic fluid systems cool, the brittle-ductile transition eventually enters the area of the deep crystalline rocks with their saline liquid phase fluids (Fig. 33). The lithostatic to hydrostatic pressure transition is the trigger that is probably episodically tripped by stresses in the system to literally fire these dense saline fluids to the high-level permeability zones. Such fluids as those at Providencia ascend so rapidly that they retain their deep-seated characteristics and are out of isotopic and chemical equilibrium with wall rocks at the site of ore deposition. There is no evidence in our isotopic data of significant entrainment of meteoric water during the ascent of the saline fluids. Instead, substantial mixing occurs only in the shallow parts of the system. There is also no evidence in our examples that either liquid or vapor-phase fluids come directly from the water-rich carapace of the magma to make epithermal ore deposits. The iso-

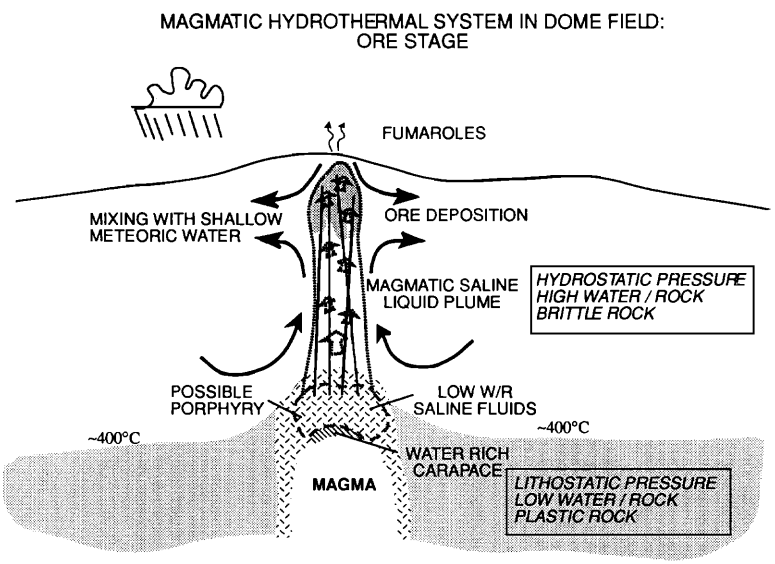

FIG. 33. Model of high-level magmatic hydrothermal system in dome field showing relationship of ore-stage saline magmatic fluids to the water-saturated carapace of the magma and the brittle-ductile transition and mixing with shallow meteoric water.

tope fractionations due to degassing of the magma chamber, H_2 loss, and possibly deep boiling that have been recognized in fluids near the carapace of some magmas do not normally reach the epithermal environment. Equilibration of the fluids with the deep crystalline rocks wipes the slate clean. As far as stable isotope geochemistry is concerned, the deep crystalline rocks between the brittle-ductile transition and the water-rich carapace of the magma can be viewed as a major reservoir of evolved magmatic fluids for epithermal ore deposits.

REFERENCES

Beaty, D. W., Cunningham, C. G., Rye, R. O., Steven, T. A., and Gonzalez-Urien, E., 1986, Geology and geochemistry of the Deer Trail Pb-Zn-Ag-Cu manto deposits, Marysvale district, west-central Utah: ECON. GEOL., v. 81, p. 1932–1952.

Benavides, J. D., 1983, Wall-rock alteration and mineralogical zoning in a section of the Julcani mining district, Peru: Unpub. M.S. thesis, Stanford Univ., 199 p.

Bove, D. J., 1988, Evolution of the Red Mountain alunite deposit, Lake City caldera, San Juan Mountains, Colorado: Unpub. M.S. thesis, Univ. Colorado, 179 p.

Bove, D. J., and Hon, K., 1990, Compositional changes induced by hydrothermal alteration at the Red Mountain alunite deposit, Lake City, Colorado: U. S. Geol. Survey Bull. 1936, 21 p.

Bove, D. J., Rye, R. O., and Hon, K., 1990, Evolution of the Red Mountain alunite deposits, Lake City, Colo: U. S. Geol. Survey Open-File Rept. 90-0235, 29 p.

Bruha, D. K., and Noble, D. C., 1983, Hypogene quartz-alunite ± pyrite alteration formed by moderately saline, ascendant hydrothermal solutions [abs.]: Geol. Soc. America Abstracts with Programs, v. 20, p. 325.

Burnham, C. W., 1979, Magmas and hydrothermal fluids, *in* Barnes, H. L., ed., Geochemistry of hydrothermal ore deposits: New York, Wiley Intersci., p. 236–277.

Burnham, C. W., and Ohmoto, H., 1980, Late stage processes of felsic magmatism: Soc. Mining Geologists Japan, Special Issue 8, p. 1–11.

Carten, R. B., Rye, R. O., and Landis, G. P., 1988, Effects of igneous and hydrothermal processes on the compositions of ore-forming fluids: Stable isotope and fluid inclusion evidence, Henderson molybdenum deposit, Colorado [abs.]: Geol. Soc. America Abstracts with Programs, v. 20, p. A94.

Cunningham, C. G., Rye, R. O., Steven, T. A., and Mehnert, H. H., 1984, Origins and exploration significance of replacement and vein-type alunite deposits in the Marysvale volcanic field, west central Utah: ECON. GEOL., v. 79, p. 50–71.

Deen, J. A., 1990, Hydrothermal ore deposition related to high-level igneous activity: A stable-isotope study of the Julcani mining district, Peru: Unpub. Ph.D. thesis, Univ. Colorado, 246 p.

Deen, J. A., Drexler, J. W., Rye, R. O., and Munoz, J. L., 1987, A magmatic fluid origin for the Julcani district, Peru: Stable isotope evidence [abs.]: Geol. Soc. America Abstracts with Programs, v. 19, p. 638.

Deen, J. A., Rye, R. O., and Drexler, J. W., 1988, Polyminerallic mineralization related to magma evolution and magmatic-meteoric fluid mixing, Julcani district, Peru [abs.]: Geol. Soc. America Abstracts with Programs, v. 19, p. A351.

Drexler, J. W., 1982, Mineralogy and geochemistry of Miocene volcanic rocks genetically associated with the Julcani Ag-Bi-Pb-Cu-Au-W deposit, Peru: Physiochemical conditions of a productive magma body: Unpub. Ph.D. thesis, Michigan Tech. Univ. 259 p.

Drexler, J. W., and Munoz, J. L., 1988, Abundances and migration of volatiles in oxidized, pyrrhotite-anhydrite-bearing silicic volcanics: Julcani, Peru: Canadian Inst. Mining Metallurgy Spec. Vol. 39, p. 10–22.

Fournier, R. O., 1983, Active hydrothermal systems as analogues of fossil systems: Geothermal Resources Council Spec. Rept. 13, p. 263–284.

—— 1985, The behavior of silica in hydrothermal solutions: Rev. Econ. Geology, v. 2, p. 45–61.

—— 1987, Conceptual models of brine evolution: U. S. Geol. Survey Prof. Paper 1350, v. 2, p. 1487–1506.

—— 1991, The transition from hydrostatic to greater than hydrostatic fluid pressure in presently active continental hydrothermal systems in crystalline rock: Geophys. Research Letters, v. 18, p. 955–958.

—— 1992, The influences of depth of burial and the brittle-plastic transition on the evolution of magmatic fluids: Japan Geol. Survey Rept. 279, p. 57–59.

Gerlach, T. E., 1993, Oxygen buffering of Kilauea volcanic gases and the oxygen fugacity of Kilauea basalt: Geochim et. Cosmochim. Acta, v. 57, p. 795–814.

Goodell, P. C., and Petersen, U., 1974, Julcani mining district, Peru: A study of metal ratios: ECON. GEOL., v. 69, p. 347–361.

Henley, R. W., and Ellis, A. J., 1983, Geothermal systems ancient and modern: A geochemical review: Earth-Sci. Rev., v. 19, p. 1–50.

Henley, R. W., and McNabb, A., 1978, Magmatic vapor plumes and ground-water interaction in porphyry copper emplacement: ECON. GEOL., v. 73, p. 1–20.

Holland, H. D., 1965, Some applications of thermochemical data to problems of ore deposits, II. Mineral assemblages and the composition of ore-forming fluids: ECON. GEOL., v. 60, p. 1101–1166.

Kelly, W. C., and Rye, R. O., 1979, Fluid inclusion and stable isotope studies of the Panasquiera tin tungsten deposit, Portugal: ECON. GEOL., v. 74, p. 1721–1822.

Landis, G. P., and Rye, R. O., 1974, Geologic fluid inclusion and stable isotope studies of the Pasto Bueno tungsten base metal deposit, northern Peru: ECON. GEOL., v. 69, p. 1025–1059.

Lipman, P. W., and Friedman, I., 1975, Interaction of meteoric water with magma: An oxygen isotope study of ash-flow sheets from southern Nevada: Geol. Soc. America Bull., v. 86, p. 695–702.

Lister, C. R. B., 1974, On the penetration of water into hot rock: Royal Astron. Soc. Geophys. Jour., v. 39, p. 465–509.

—— 1980, Heat flow and hydrothermal circulation: Ann. Rev. Earth Planet. Sci., v. 8, p. 95–117.

Matsuhisa, Y., 1992, Origin of magmatic waters in subduction zones: Stable isotope constraints: Japan Geol. Survey Rept. 279, p. 104–109.

Noble, D. C., and Silberman, M. L., 1984, Evolution volcanica e hidrotermal y cronologia de K-Ar del distrito minero de Julcani, Peru: Soc. Geol. Peru, Vol. Jubilar, 60th Anniv., pt. 5, p. 1–35.

Ohmoto, H., 1986, Stable isotope geochemistry of ore deposits: Rev. Mineralogy, v. 16, p. 491–560.

Ohmoto, H., and Lasaga, A. C., 1982, Kinetics of reactions between aqueous sulfates and sulfides in hydrothermal systems: Geochim et. Cosmochim. Acta, v. 46, p. 1727–1746.

Ohmoto, H., and Rye, R. O., 1974, Hydrogen and oxygen isotopic compositions of fluids inclusions in the kuroko deposits, Japan: ECON. GEOL., v. 69, p. 947–953.

—— 1979, Isotopes of sulfur and carbon, *in* Barnes, H. L., ed., Geochemistry of hydrothermal ore deposits: New York, Wiley Intersci., p. 509–567.

Petersen, U., Noble, D. C., Arenas, M. J., and Goodell, P. C., 1977, Geology of the Julcani mining district, Peru: ECON. GEOL., v. 72, p. 931–949.

Rye, R. O., 1966, Carbon, hydrogen, and oxygen isotopic composition of the hydrothermal fluids responsible for the Pb-Zn deposits at Providencia, Zacatecas, Mexico: ECON. GEOL., v. 61, p. 1399–1427.

Rye, R. O., and Sawkins, F. J., 1974, Fluids inclusion and stable isotope studies of the Casapalca Ag-Pb-Zn-Cu deposit, central Andes, Peru: ECON. GEOL., v. 69, p. 181–205.

Rye, R. O., Hall, W. E., and Ohmoto, H., 1974, Carbon, hydrogen, oxygen and sulfur isotope study of the Darwin silver-lead-zinc deposit, southern California: ECON. GEOL., v. 69, p. 293–317.

Rye, R. O., Stoffregen, R. E., and Bethke, P. M., 1990, Stable isotope systematics and magmatic hydrothermal processes in the Summitville, CO gold deposit: U. S. Geol. Survey Open-File Rept. 90-626, 31 p.

Rye, R. O., Bethke, P. M., and Wasserman, M. D., 1992, The stable isotope geochemistry of acid sulfate alteration: ECON. GEOL., v. 87, p. 225–262.

Sawkins, F. J., 1964, Lead-zinc ore deposition in the light of fluid inclusion studies, Providencia mine, Zacatecas, Mexico: ECON. GEOL., v. 59, p. 883–919.

Shelnutt, J. P., and Noble, D. C., 1985, Premineralization radial dikes of tourmalinized fluidization breccia, Julcani district, Peru: ECON. GEOL., v. 80, p. 1622–1632.

Steven, T. A., and Ratte, J. C., 1960, Geology and ore deposits of the Summitville district, San Juan Mountains, Colorado: U. S. Geol. Survey Prof. Paper 487, 90 p.

Stoffregen, R., 1987, Genesis of acid sulfate alteration and Au-Cu-Ag mineralization at Summitville, Colorado: ECON. GEOL., v. 82, p. 1575–1591.

Taylor, B. E., 1992, Hydrogen isotope composition of magmatic water [abs.]: Geol. Soc. America Abstracts with Programs, v. 24, p. A145.

Taylor, B. E., Eichelberger, J. C., and Westrich, H. R., 1983, Hydrogen isotopic evidence of rhyolitic magma degassing during shallow intrusion and eruption: Nature, v. 306, p. 541–545.

Taylor, H. P., Jr., 1979, Oxygen and hydrogen isotope relationships in hydrothermal mineral deposits, *in* Barnes, H. L., ed., Geochemistry of hydrothermal ore deposits: New York, Wiley Intersci., p. 236–277.

—— 1986, Igneous rocks II. Isotopic case studies of circumpacific magmatism. Stable isotopes in high temperature geological processes: Rev. Mineralogy, v. 16, p. 273–318.

Whitney, J. A., 1988, Composition and activity of sulfurous species in quenched magmatic gases associated with pyrrhotite-bearing silicic magmas: ECON. GEOL., v. 83, p. 86–92.